

Monitoring Water Quality of Inland Lakes using Remote Sensing

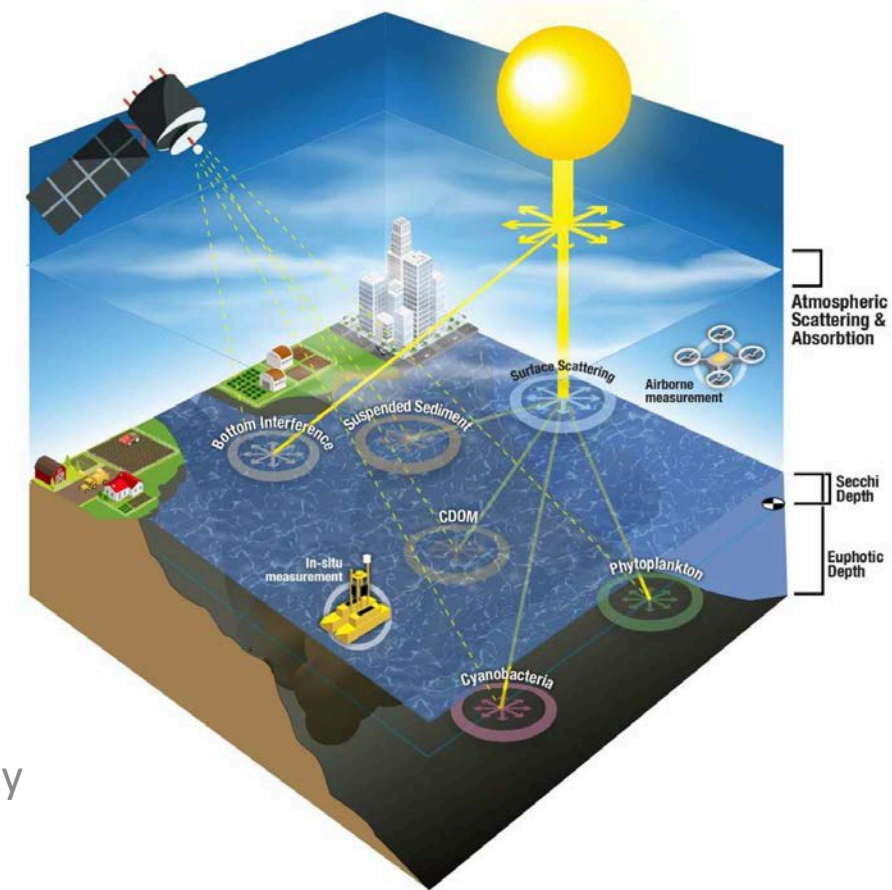
Marzi Azarderakhsh

Associate Professor

Department of Construction Management & Civil Engineering | CUNY | City Tech | Brooklyn, NY

E: maazarderakhsh@citytech.cuny.edu

Zoom: <https://us02web.zoom.us/my/mazarderakhsh>



Kickoff meeting for Summer Bridge/REU program
June 2023

Harmful Algal Blooms (HABs)

Uncontrolled growth of algae that negatively impact aquatic ecosystems

- Runoff from agriculture, storm systems, poor water circulation, and extreme weather events

High concentrations of algae can:

- Suppress oxygen supply to organisms
- Release toxins into ecosystem
- Prevent surrounding recreational and economic aquaculture



What causes HABs?

- Nutrient loading “eutrophication”
- Pollution
- Warm water
- Food web changes
- Introduced species
- Changes in water flow
 - e.g., after major events like hurricanes, drought, or floods
- Other, yet unknown, factors

What is Harmful Algal Bloom?

- *“Harmful algal blooms, or HABs, occur when colonies of algae — simple plants that live in the sea and freshwater — grow out of control and produce toxic or harmful effects on people, fish, shellfish, marine mammals and birds. The human illnesses caused by HABs, though rare, can be debilitating or even fatal.”*



HABs Detection

Field Studies

- Expensive
- Time consuming laboratory analysis
- Detection of toxin concentrations through in situ sampling
- Labor intensive



Satellite Sensing

- Extensive coverage of waterbody
- Tracks spatiotemporal algal distribution
- Not yet well studied
- Everything is at the research level, not the applied level



Why Satellite based monitoring?

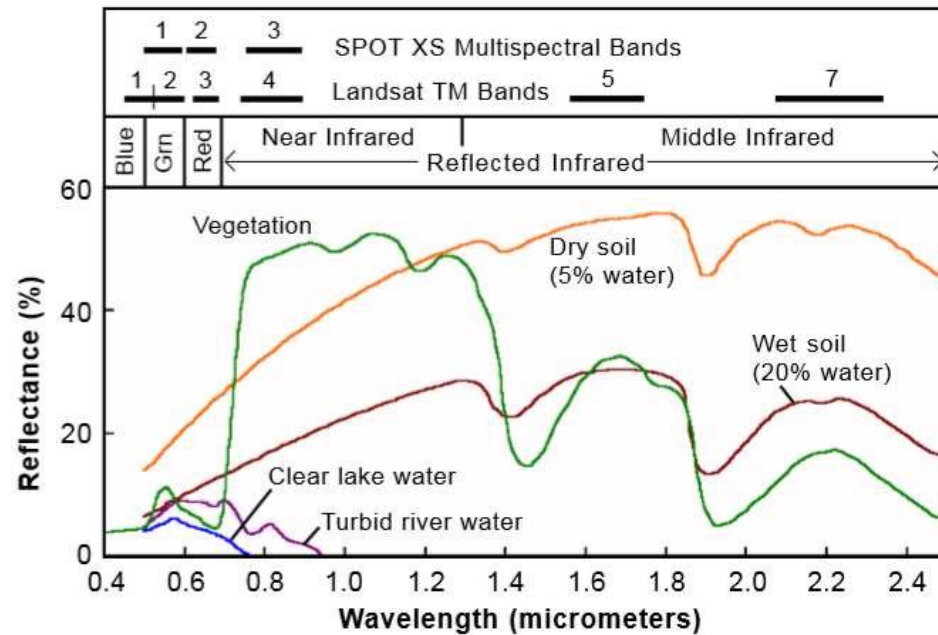
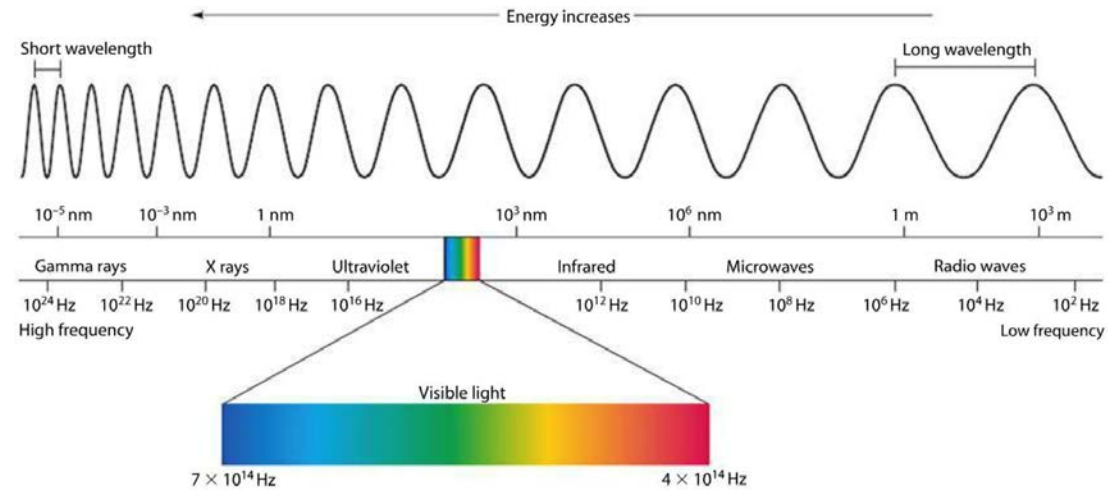
- The intensity of HAB
- Geographic distribution.
- Temporal pattern of blooms
- Access to lakes not currently monitored



The most commonly measured qualitative parameters of water by means of remote sensing

Water Quality Parameter	Abbreviation	Units
chlorophyll- <i>a</i>	CHL- <i>a</i>	mg/L
Secchi Disk Depth	SDD	m
Temperature	T	°C
Colored Dissolved Organic Matters	CDOM	mg/L
Total Organic Carbon	TOC	mg/L
Dissolved Organic Carbon	DOC	mg/L
Total Suspended Matters	TSM	mg/L
Turbidity	TUR	NTU
Sea Surface Salinity	SSS	PSU
Total Phosphorus	TP	mg/L
Ortho-Phosphate	PO ₄	mg/L
Chemical Oxygen Demand (COD)	COD	mg/L
Biochemical Oxygen Demand	BOD	mg/L
Electrical Conductivity	EC	μs/cm
Ammonia Nitrogen	NH ₃ -N	mg/L

Electromagnetic Radiation Spectrum



(Mondal, 2018)

Applications of Remote Sensing for Lakes

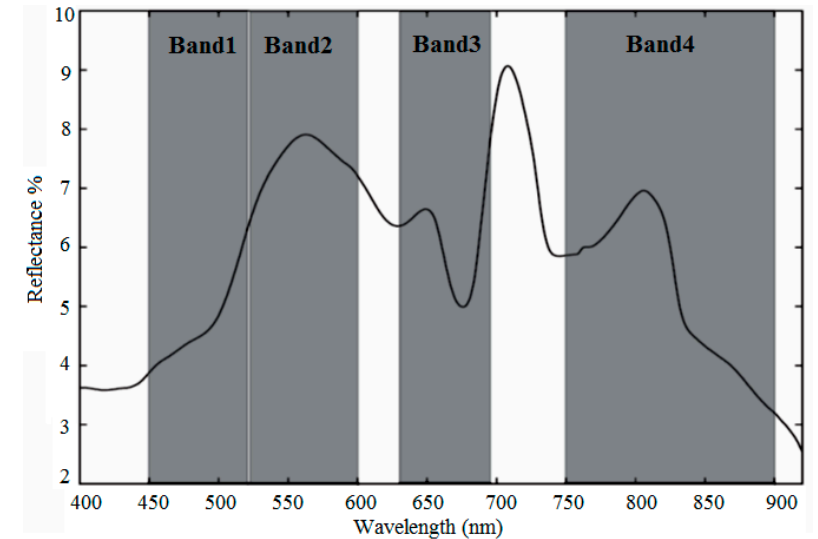
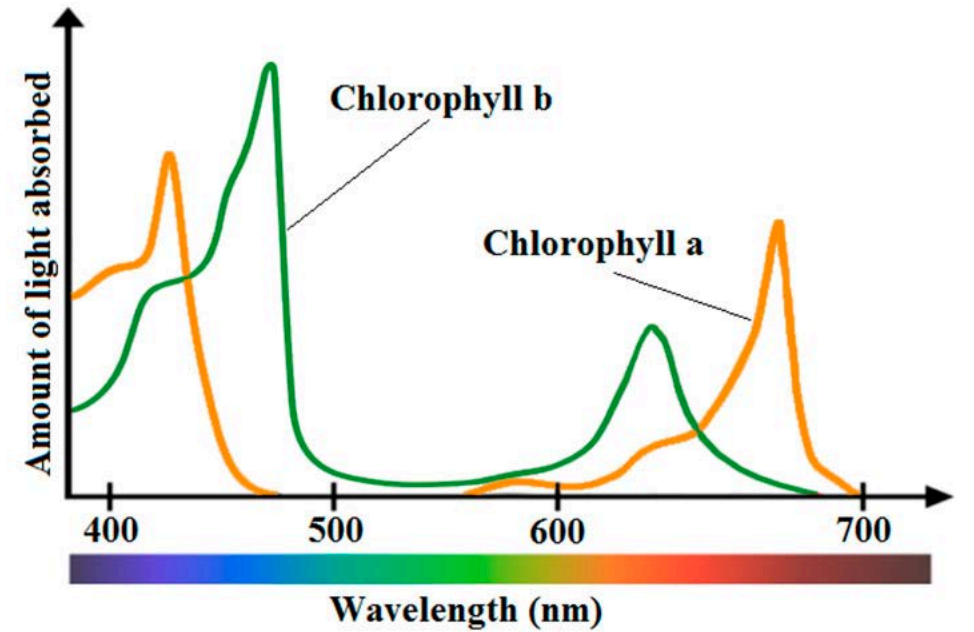
Table 1. Available satellites for remote sensing water quality retrieval (bands more than 5).

	Satellite Sensor	Launch Date	Spatial Resolution (m)	Spectral Resolution Band	Temporal Resolution (Day)
Multi-spectral	NIMBUS-7 CZCS	1978.10	825	6	6
	Landsat-5/7/8/9	1984–2020	30	5	16
	SeaWiFS	1997.8	1130	8	16
	NOAA-16 AVHRR	2000.10	1100–4000	6	9
	EO-1 ALI	2000.11	10	9	16
	WorldView-2/3	2009/2014	1.85/1.24	8	1.1
	MERIS	2002.3	300–1200	15	1
	MODIS	1999.12	250–500–1000	9	0.5
	Landsat-8 OLI	2013.2	30	7	16
Hyper-spectral	HY-1A COCTS	2002.5	1100	10	3
	PROBA CHRIS	2001.10	18–36	19	7
	Hyperion	2000.11	30	42	16
	HJ-1A HSI	2008.9	100	128	4
	HICO	2009.9	100	128	10
	VIIRS	2011.10	375–750	22	0.5
	OHS	2018.4	10	32	2
	GF5-AHSI	2018.5	30	330	3
	ZY1-02D	2019.9	30	166	3
sensors for UAV	ZK-VNR-FPG480	/	0.09	270	/
	GaiaSky-mini	/	0.04	176	/

Yang, H.; Kong, J.; Hu, H.; Du, Y.; Gao, M.; Chen, F. A Review of Remote Sensing for Water Quality Retrieval: Progress and Challenges. *Remote Sens.* 2022, 14, 1770. <https://doi.org/10.3390/rs14081770>

Chl-a

Band Combination	Sensor
Ratio between green (0.50–0.60 μm) and red (0.60–0.70 μm)	Landsat 5-TM Landsat 5-MSS Landsat 7-ETM+ SPOT IRS-LISS-III
Ratio between near infrared (NIR) and red	Landsat 5-TM HICO PROBA-CHRIS MODIS MERIS AISA
Ratio between green and blue (B2/B1)	Landsat 5-TM Landsat 7-ETM+ MERIS PROBA-CHRIS EO-1 Hyperion
Ratio between blue (0.40–0.50 μm) and red (0.60–0.70 μm)	Landsat 5-TM Landsat 7-ETM+
Using a single band	Blue (0.40–0.50 μm) Landsat 5-TM
	Red (0.60–0.70 μm) PROBA-CHRIS Landsat 5-TM CASI
	Green (0.50–0.60 μm) Landsat 5-TM Daedalus Airborne Thematic Mapper (ATM)



Spectral band positioning of Landsat7/on

List of the more commonly used spaceborne sensors in water quality assessments.

Category	Satellite—Sensor	Launch Date	Spectral Bands (nm)	Spatial Resolution (m)	Swath Width (km)	Revisit Interval (Day)
High Resolution	Digital Globe WorldView-1	18 September 2007	Pan	0.5	17.7	1.7
	Digital Globe WorldView-2	8 October 2009	8 (400–1040)-1 Pan (450–800)	1.85–0.46	16.4	1.1
	NOAA WorldView-3	13 August 2014	8 (400–1040)-1 Pan (450–800)-8 SWIR (1195–2365)	1.24–3.7–0.31	13.1	1–4.5
	Digital Globe Quickbird	18 October 2001	4 (430–918)-1 Pan (450–900)	2.62–0.65	18	2.5
	GeoEye Geoeye-1	6 September 2010	4 (450–920)-1 Pan (450–800)	1.65–0.41	15.2	<3
	GeoEye IKONOS	24 September 1999	4 (445–853)-1 Pan (526–929)	3.2–0.82	11.3	~3
	SPOT-5 HRG	4 May 2002	3 (500–890)-1 Pan (480–710)-1 SWIR (1580–1750)	2.5 and 5–10–20	60	2–3
	CARTOSAT	5 May 2005	Pan (500–850)	2.5	30	5
Moderate Resolution	ALOS AVNIR-2	24 January 2006	4 (420–890)-1 Pan (520–770)	2.5–10	70	2
	Landsat-8 OLI/TIRS	11 February 2013	5 (430–880)-1 Pan (500–680)-2 SWIR (1570–2290)-1 cirrus cloud detection (1360–1380)-2 TIRS (10,600–12,510)	30–15–100	170	16
	Landsat-7 ETM+	15 April 1999	6 (450–1750)-1 Pan (520–900)-1 (2090–2350)-1 (1040–1250)	30–15–60	183	16
	Landsat-5 TM	1 March 1984	5 (450–1750)-1 (2080–2350)-1 (1040–1250)	30–120	185	16
	Landsat-5 MSS	1 March 1984	4 (450–1750)-1 Pan (1040–1250)	80	185	18
	EO-1 Hyperion	21 November 2000	242 (350–2570)	30	7.5	16
	EO-1 ALI	21 November 2000	9(433–2350)-1 Pan (480–690)	10–30	185	16
	Terra ASTER	18 December 1999	3 VNIR (520–860)-6 SWIR (1600–2430)-5 TIR (8125–11,650)	15–30–90	60	16
	PROBA CHRIS	22 October 2001	19 in the VNIR range (400–1050)	18–36	14	7
Regional-Global Resolution	HICO	10 September 2009	128 (350–1080)	100	45–50	10
	Terra MODIS	18 December 1999	2 (620–876)-5 (459–2155)-29 (405–877 and thermal)	250–500–1000	2330	1–2
	Envisat-1 MERIS	1 March 2002	15 (390–1040)	300–1200	1150	daily
	OrbView-2 SeaWiFS	1 August 1997	8 (402–885)	1130	2806	16
	NIMBUS-7 CZCS	24 October 1978	6 (433–12,500)	825	1556	6
	ERS-1 ATSR-1	17 June 1991	1 SWIR (1600), 1 MWIR (3700), 2 TIR (10,850–12,000), Nadir-viewing Microwave Sounder with channels at 23.8 and 35.6 GHz	1000 (MW sounder: 20 km)	500	3–6
	ERS-2 ATSR-2	22 April 1995	3 VIS-NIR (555–865), 1 SWIR (1600), 1 MWIR (3700), 2 TIR (10,850–12,000)	1000	500	3–6
	ENVISAT AATSR	1 March 2002	3 VIS-NIR (555–865), 1 SWIR (1600), 1 MWIR (3700), TIR (10,850–12,000)	1000	500	3–6
	Suomi NPP VIIRS	28 October 2011	5 I-bands (640–1145), 16 M-bands (412–12,013), DNB (500–900)	375–750	3060	1–2 times a day
NOAA-16 AVHRR	21 September 2000	6 (650–1230)	1100–4000	3000	9	

Imaging Factors to Consider

Cloud Coverage

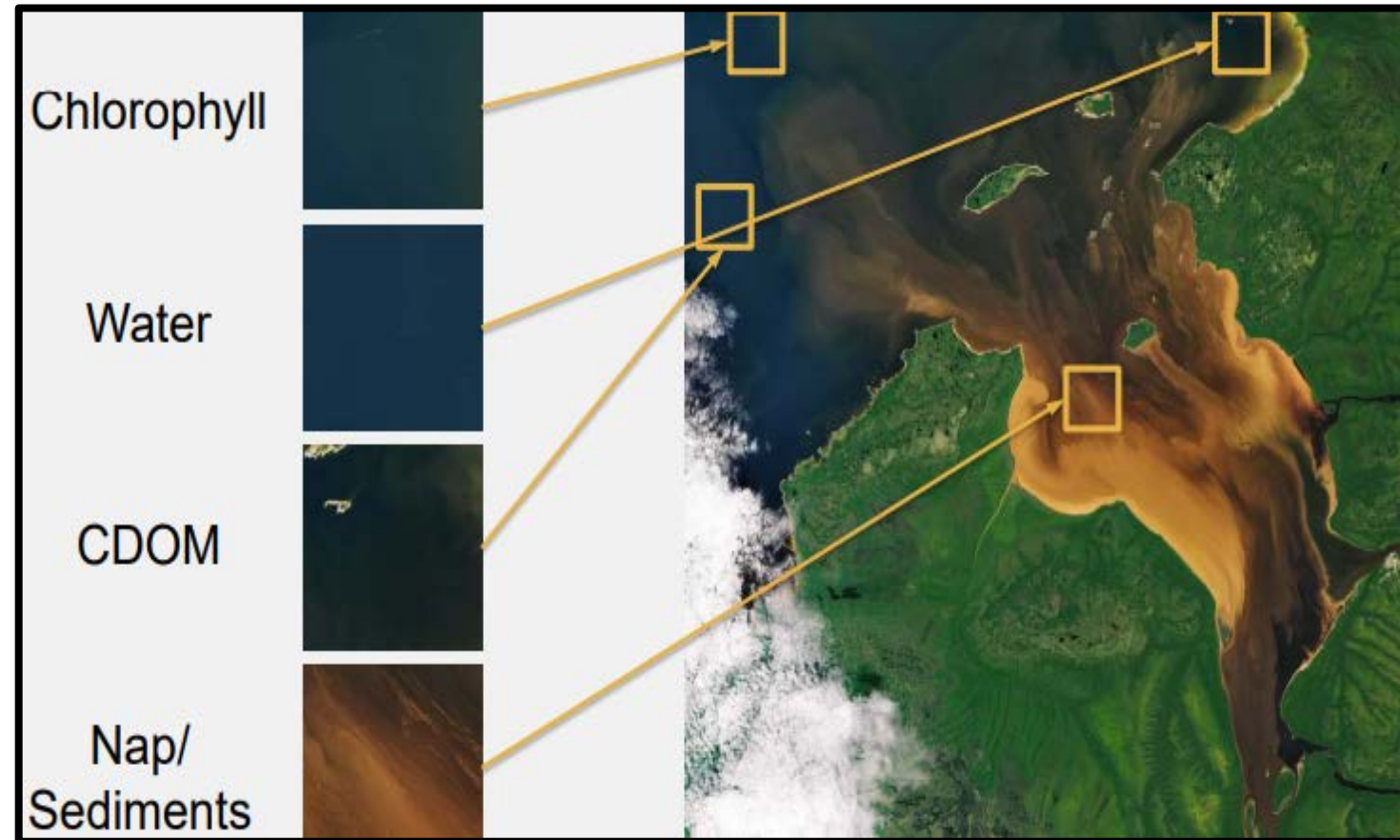
- Cloud masks
- Causes even less data for consideration
- Shadows

Spatial-temporal changes to concentration of HABs

Image resolutions

Optical or atmospheric disturbances of water

- Sedimentation
- Colored dissolved organic matter (CDOM)



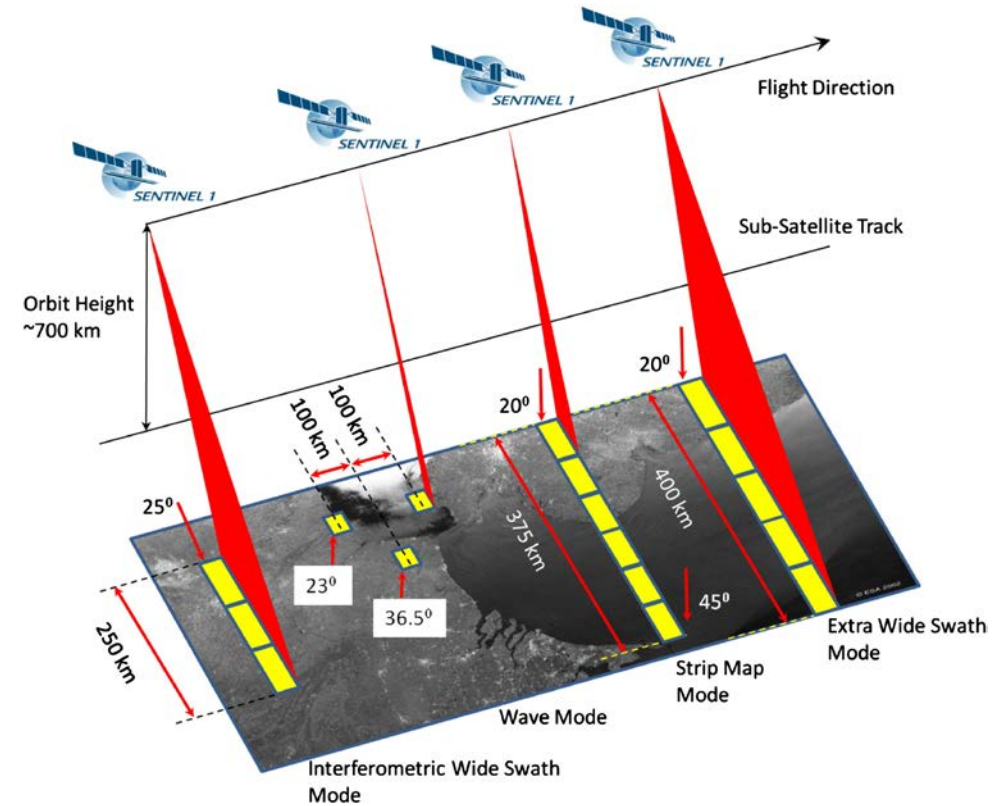
Landsat Missions

Landsat Missions: Imaging the Earth Since 1972

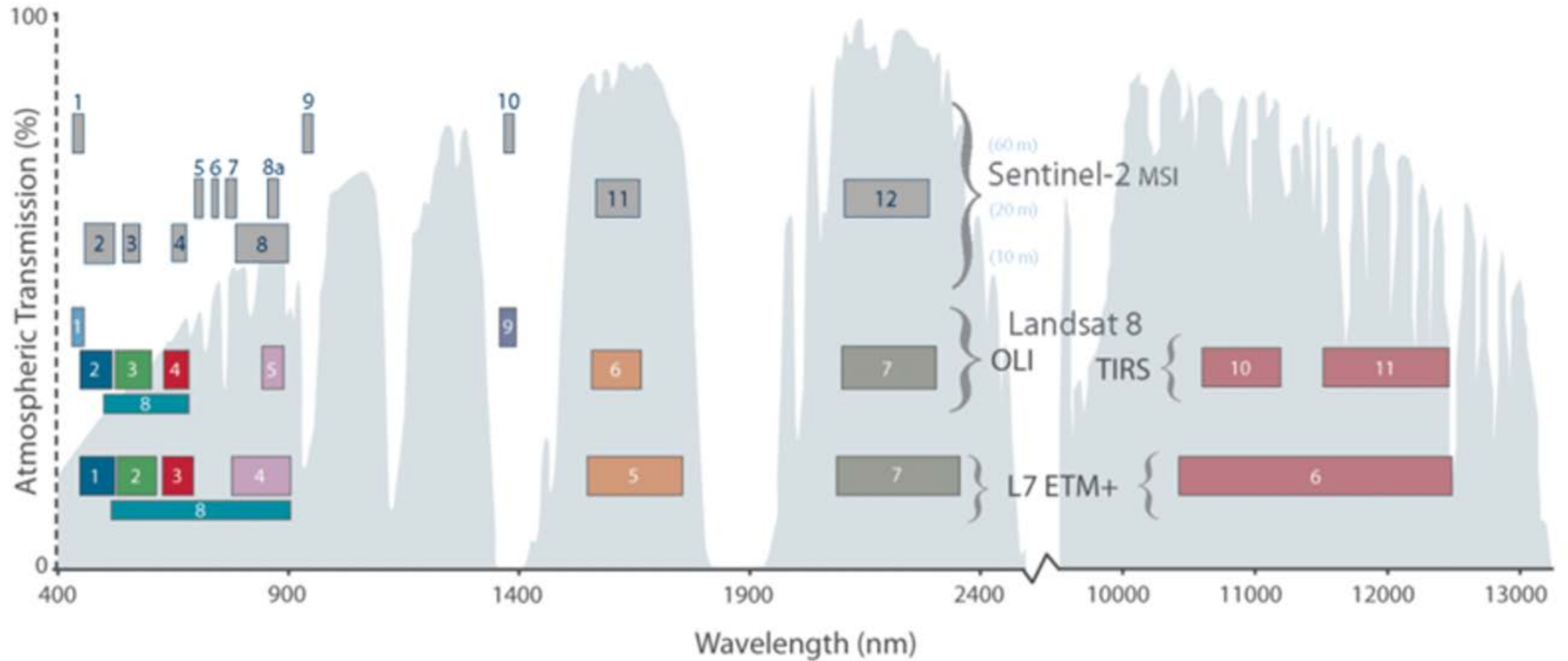


SENTINEL -1

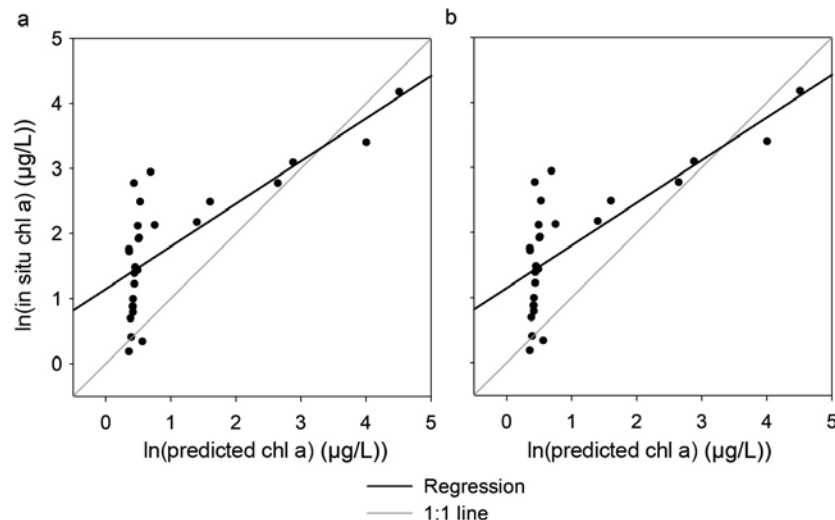
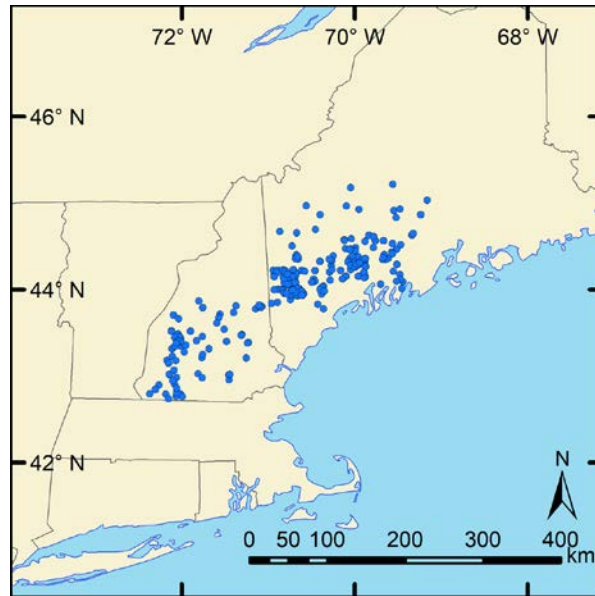
- single C-band synthetic aperture radar instrument operating at a centre frequency of 5.405 GHz.
- 12 day repeat cycle at Equator with one satellite, 175 orbits/cycle. 6-day both satellites
- Potential use: TSS, solid particle detection.



Sentinel-2



Chlorophyll-a Detection Using LandSat 8



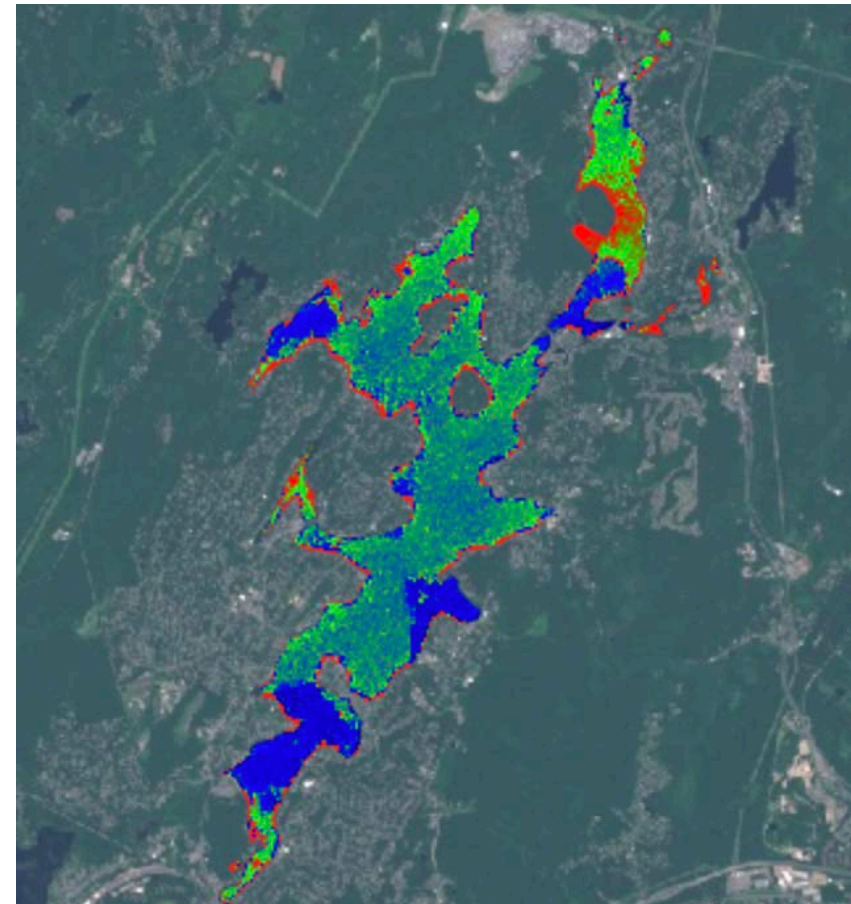
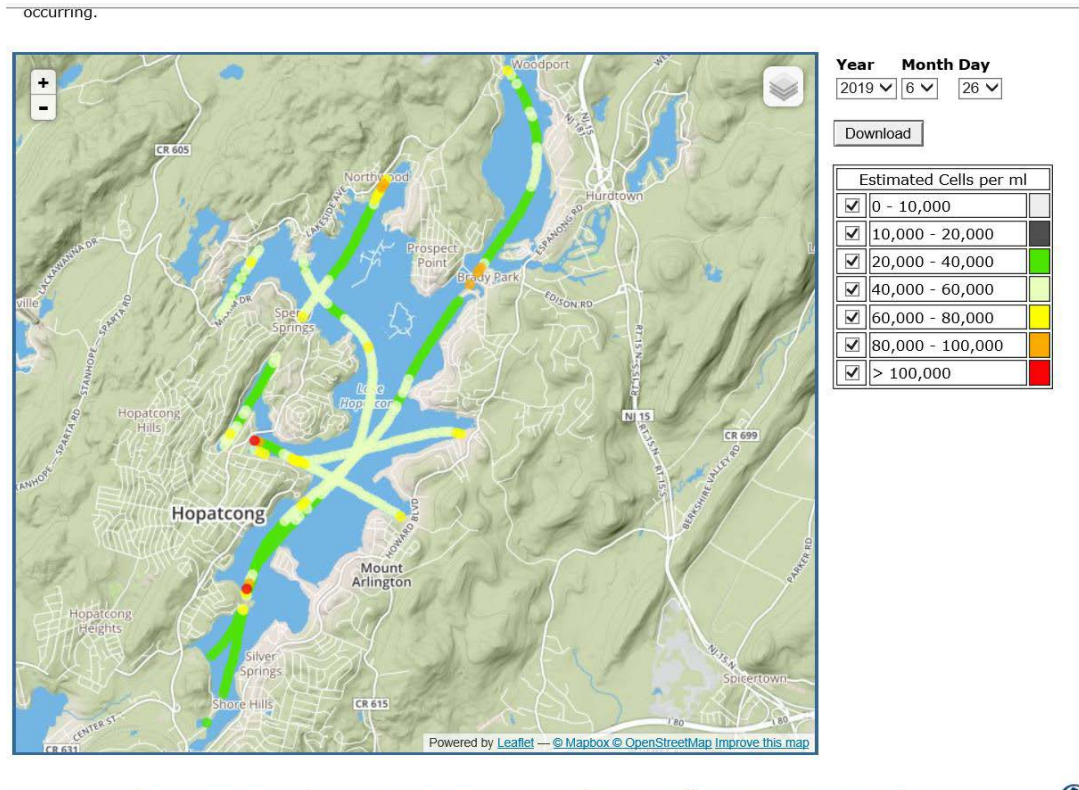
Algorithm	Landsat 8 band math	Original use	Source
Surface Algal Bloom Index (SABI)	$(B5 - B4) / (B2 + B3)$	ocean, designed to minimize variations in cloud shadow and atmospheric conditions, using MODIS satellite	Alawadi (2010)
3BDA-like (KIVU)	$(B2 - B4) / B3$	large freshwater lake, above 3 µg/L, Landsat TM	Brivio et al. (2001)
Normalized Difference Vegetation Index (NDVI)	$(B5 - B4) / (B5 + B4)$	estuarine and coastal waters 1–60 µg/L, using MERIS satellite	Mishra and Mishra (2012)
2BDA	B5/B4	simulated turbid productive freshwater, using Landsat TM	Dall’Olmo and Gitelson (2006)
Kab1	$1.67 - 3.94 \times \ln(B2) + 3.78 \times \ln(B3)$	coastal, best-fit algorithm, chl <i>a</i> below 4 µg/L, using Landsat 7	Kabbara et al. (2008)
Kab2	$6.92274 - 5.7581 \times (\ln(B1) / \ln(B3))$	coastal, best-fit algorithm, chl <i>a</i> below 4 µg/L, using Landsat 7	Kabbara et al. (2008)

Boucher, J., Weathers, K.C., Norouzi, H. and Steele, B. (2018), Assessing the effectiveness of Landsat 8 chlorophyll *a* retrieval algorithms for regional freshwater monitoring. *Ecol Appl*, 28: 1044-1054.

<https://doi.org/10.1002/eap.1708>

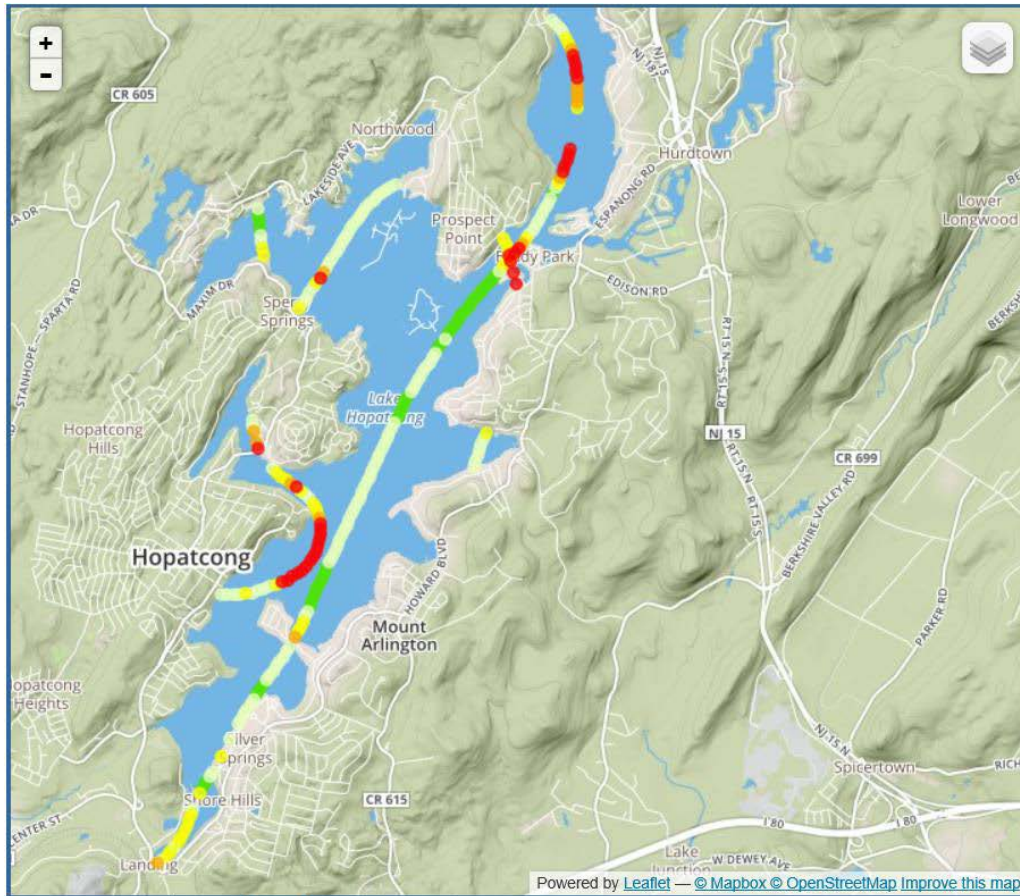
HABs Monitoring Using Sentinel-2

Lake Hopatcong. June, 2019



HABs Monitoring Using Sentinel-2

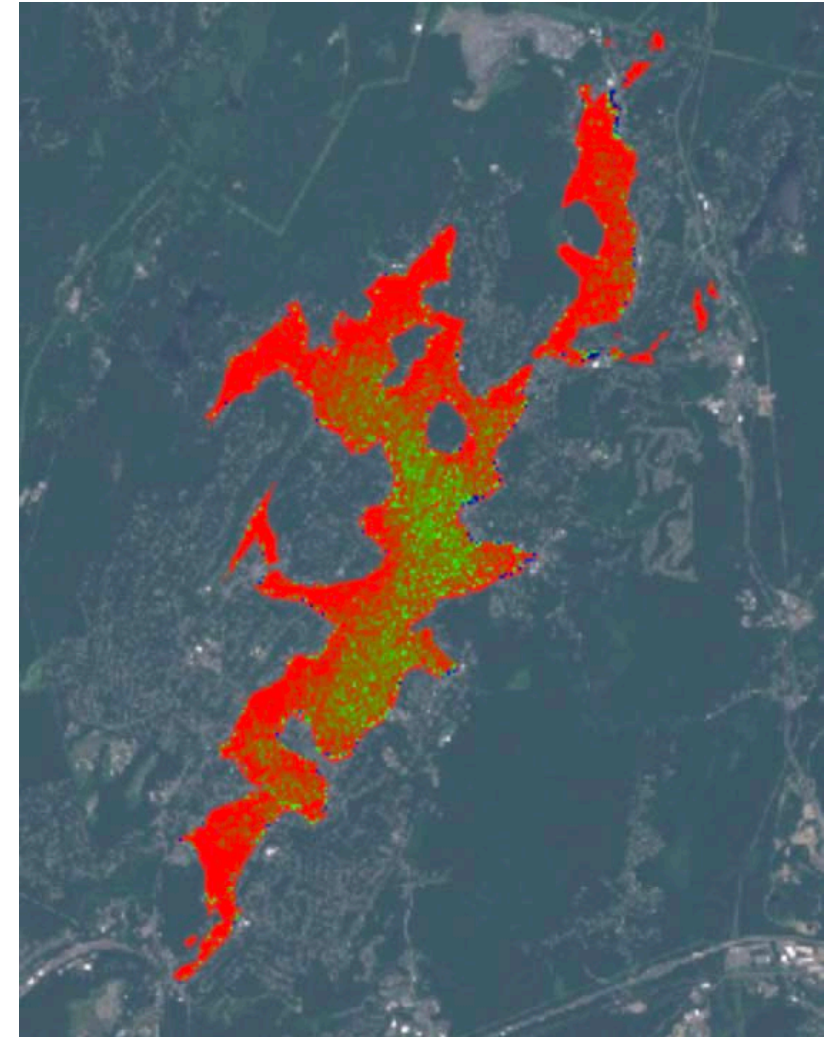
Lake Hopatcong. July, 2019



Year Month Day
2019 7 24

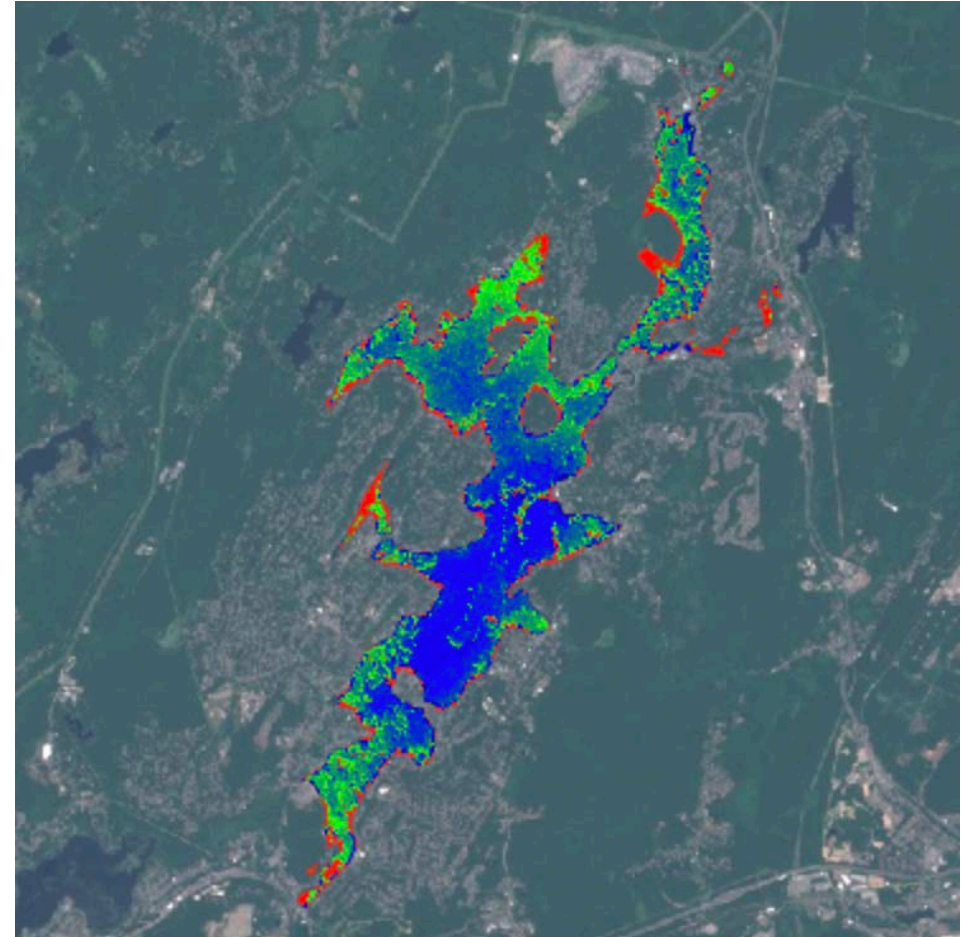
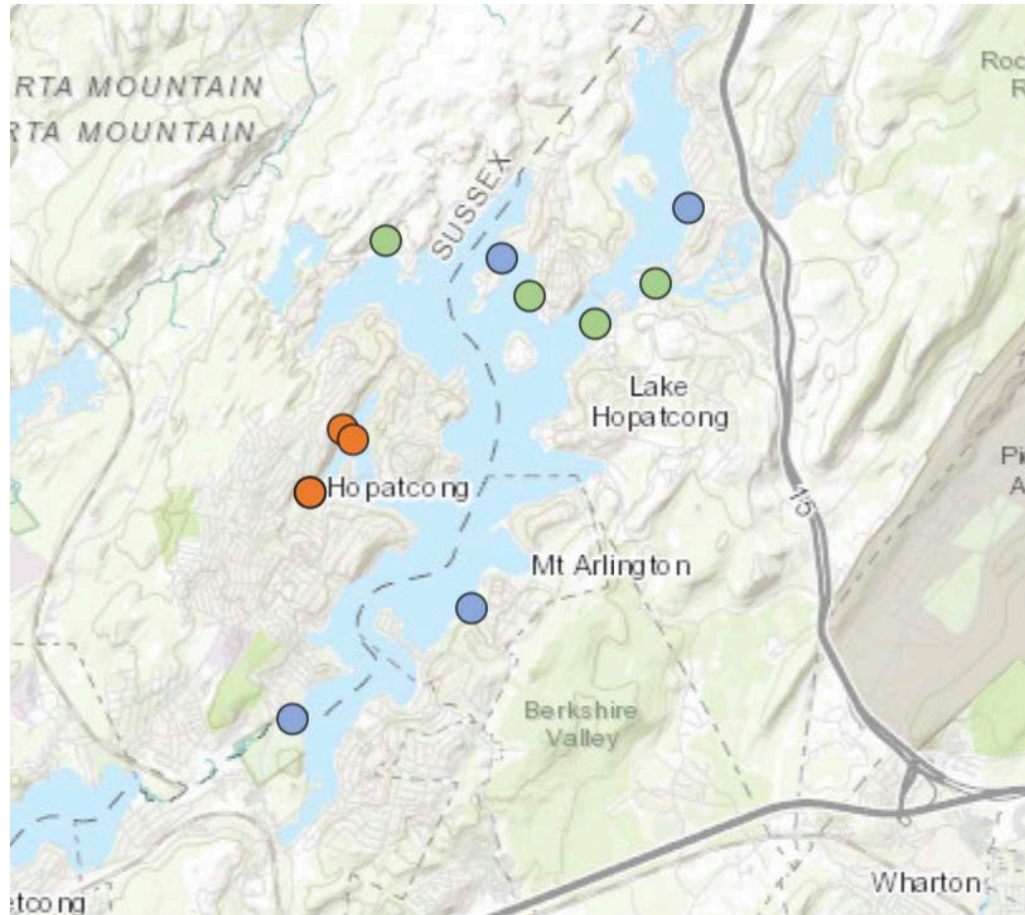
Download

Estimated Cells per ml	
<input checked="" type="checkbox"/>	0 - 10,000
<input checked="" type="checkbox"/>	10,000 - 20,000
<input checked="" type="checkbox"/>	20,000 - 40,000
<input checked="" type="checkbox"/>	40,000 - 60,000
<input checked="" type="checkbox"/>	60,000 - 80,000
<input checked="" type="checkbox"/>	80,000 - 100,000
<input checked="" type="checkbox"/>	> 100,000



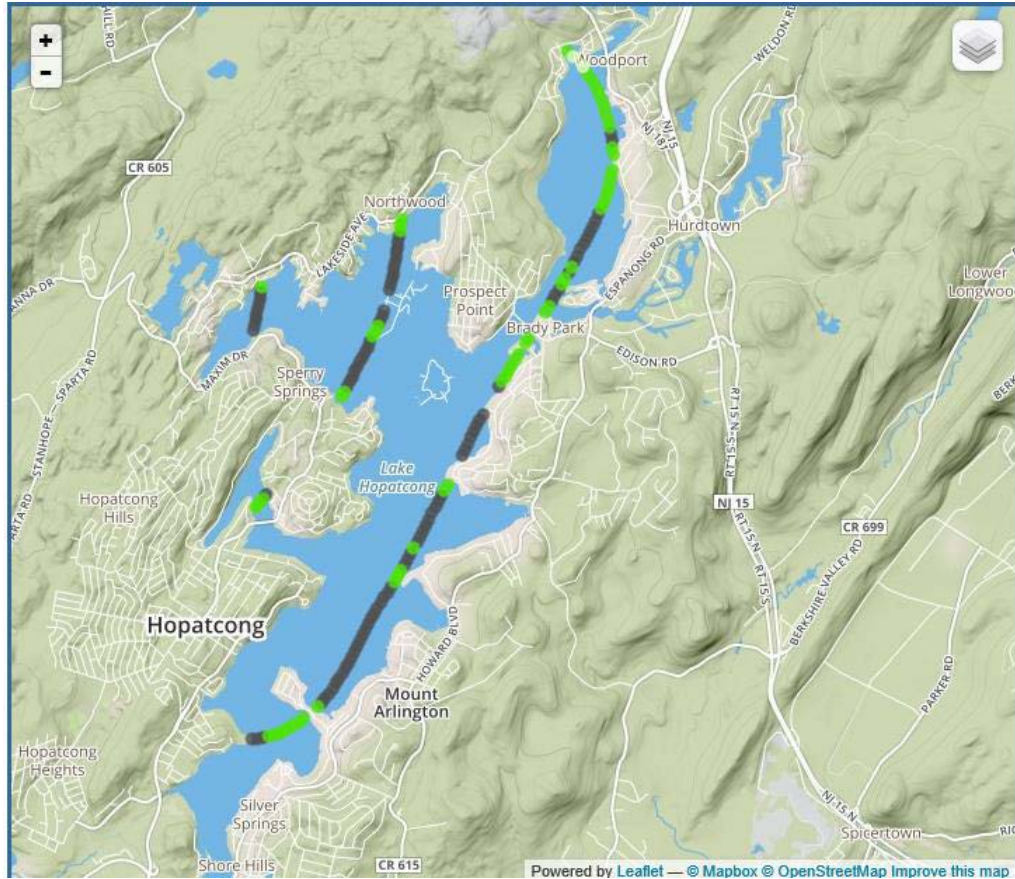
HABs Monitoring Using Sentinel-2

Lake Hopatcong. July, 2020



HABs Monitoring Using Sentinel-2

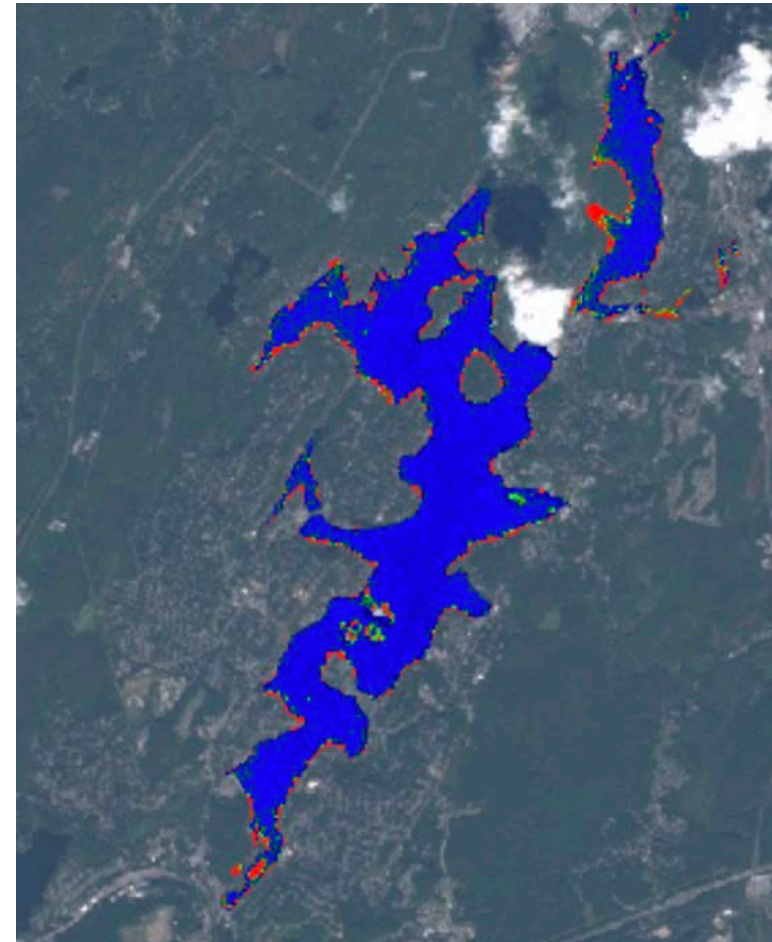
Lake Hopatcong. September, 2019



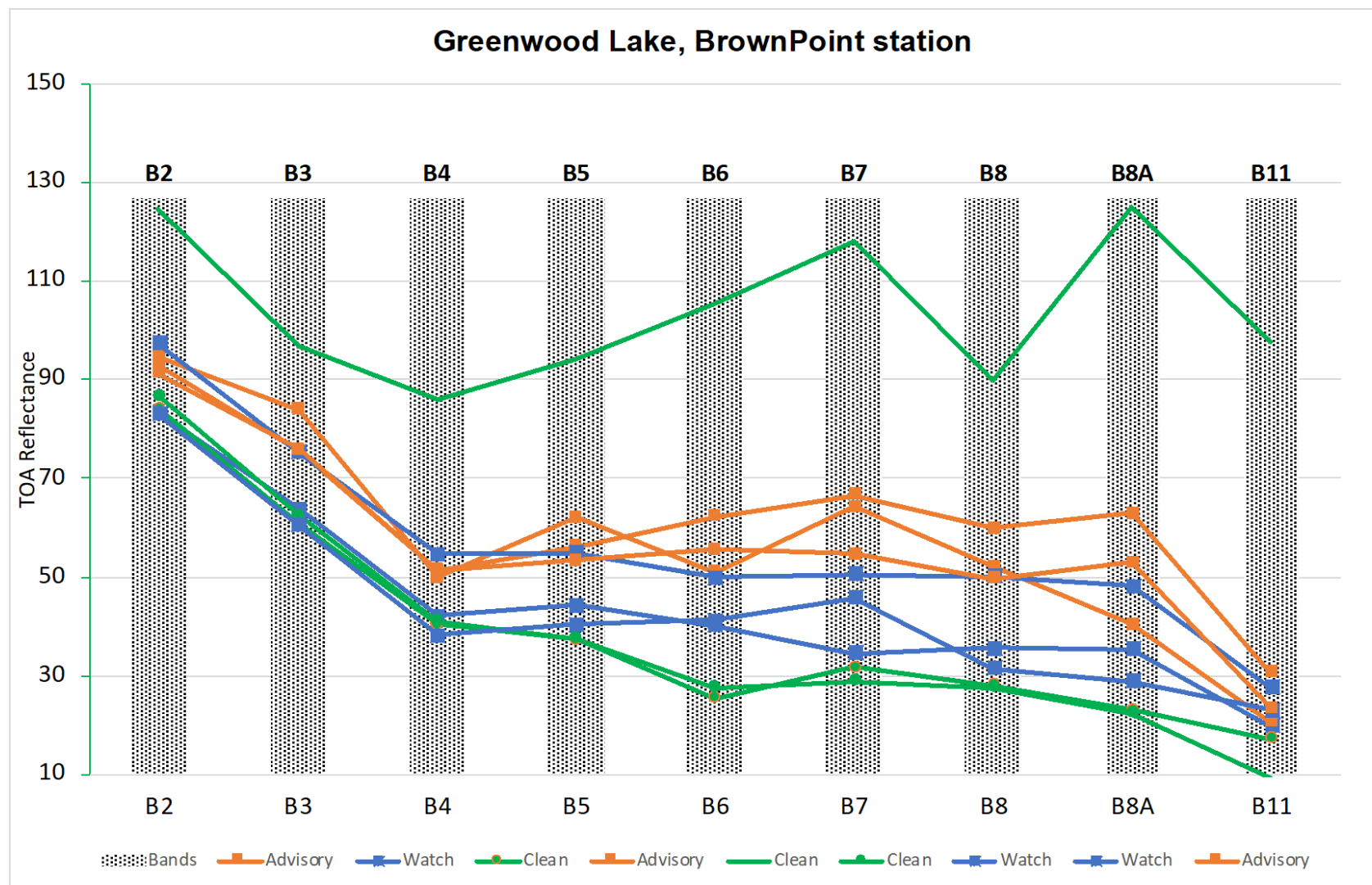
Year: 2019 | Month: 9 | Day: 24

Download

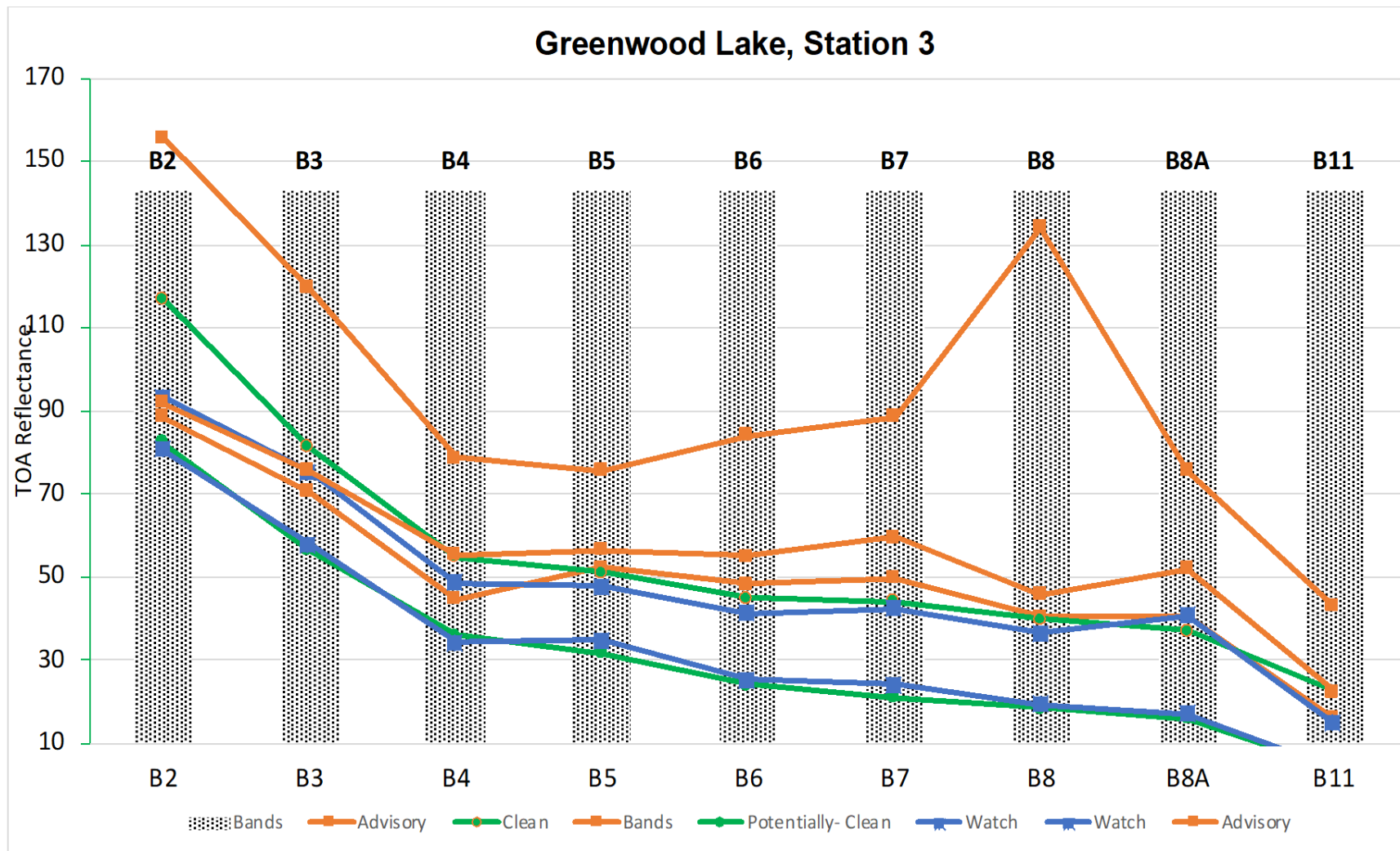
Estimated Cells per ml	
<input checked="" type="checkbox"/>	0 - 10,000
<input checked="" type="checkbox"/>	10,000 - 20,000
<input checked="" type="checkbox"/>	20,000 - 40,000
<input checked="" type="checkbox"/>	40,000 - 60,000
<input checked="" type="checkbox"/>	60,000 - 80,000
<input checked="" type="checkbox"/>	80,000 - 100,000
<input checked="" type="checkbox"/>	> 100,000



HABs Monitoring – Spectral Analysis



HABs Monitoring – Spectral Analysis



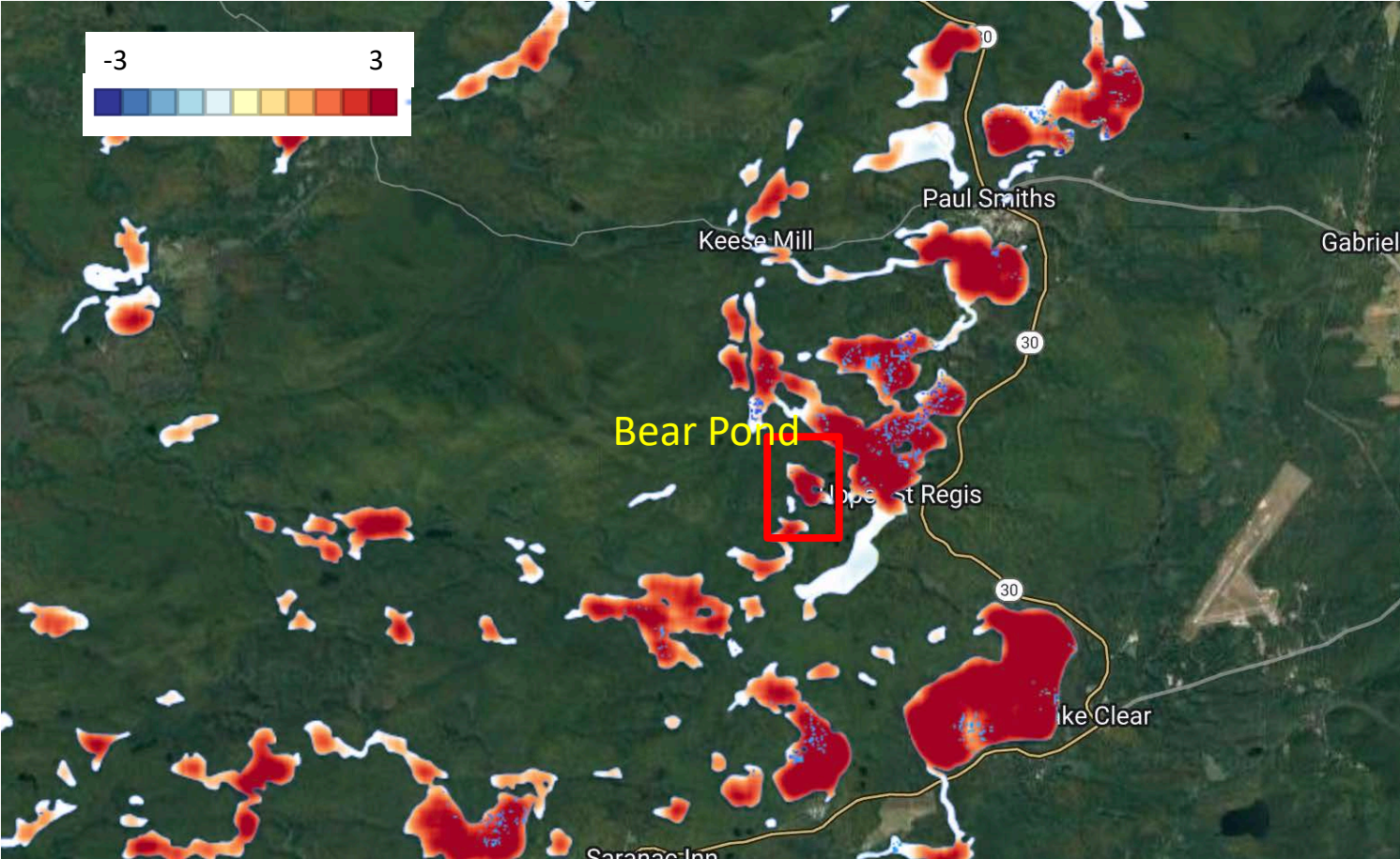
Lake Color change

- Bear pond,
Adirondack State
Park

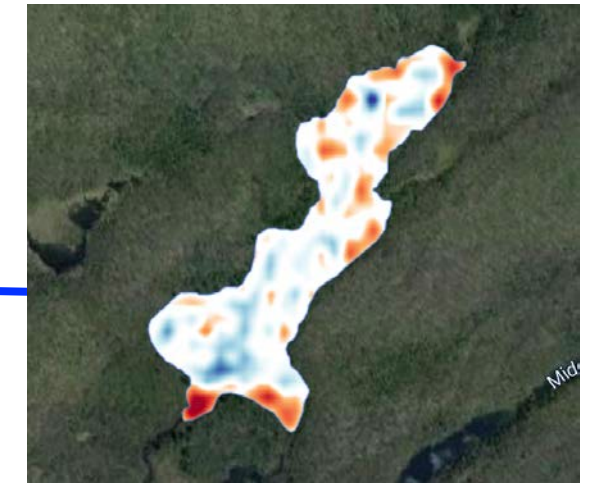
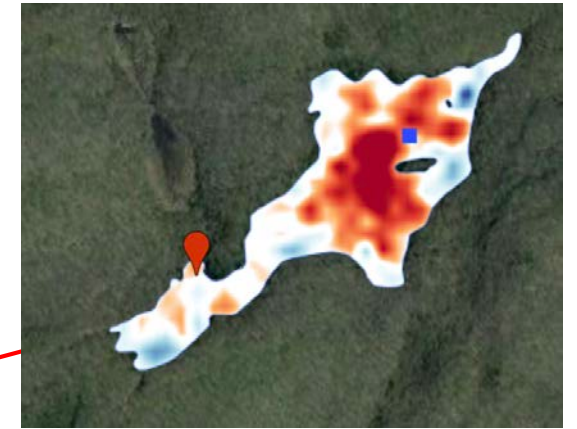
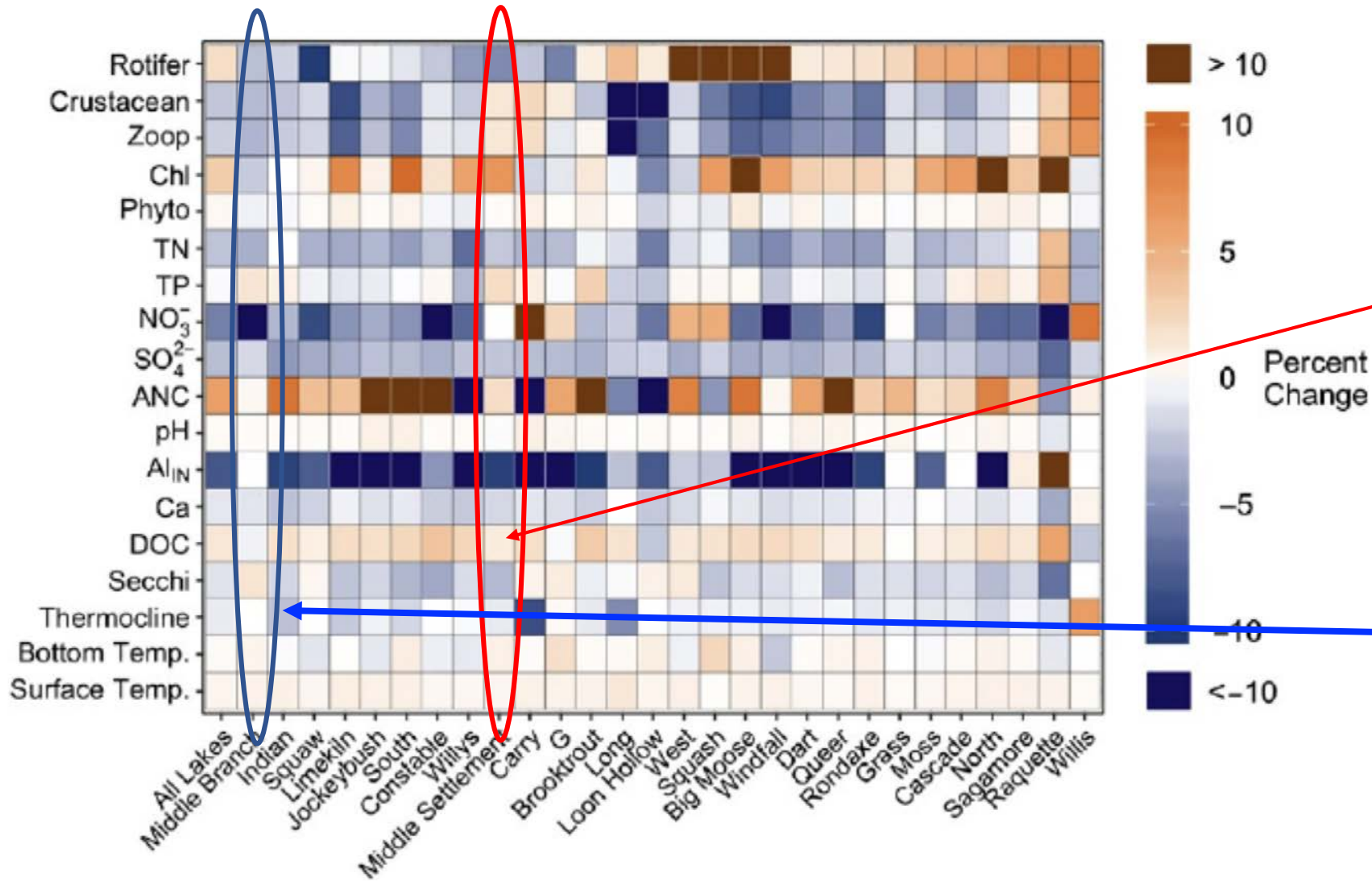


(Credit: Curt Stager)

CDOM Difference between 2020 and 2000



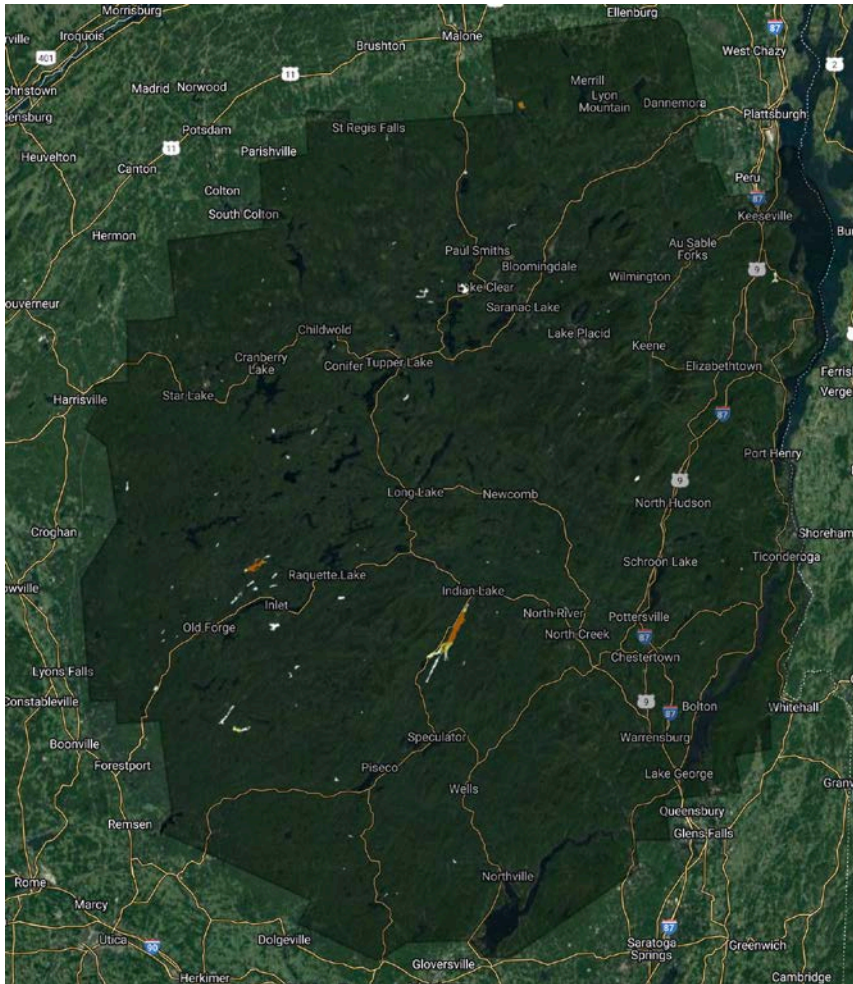
Comparison with AEAP sampling lake results



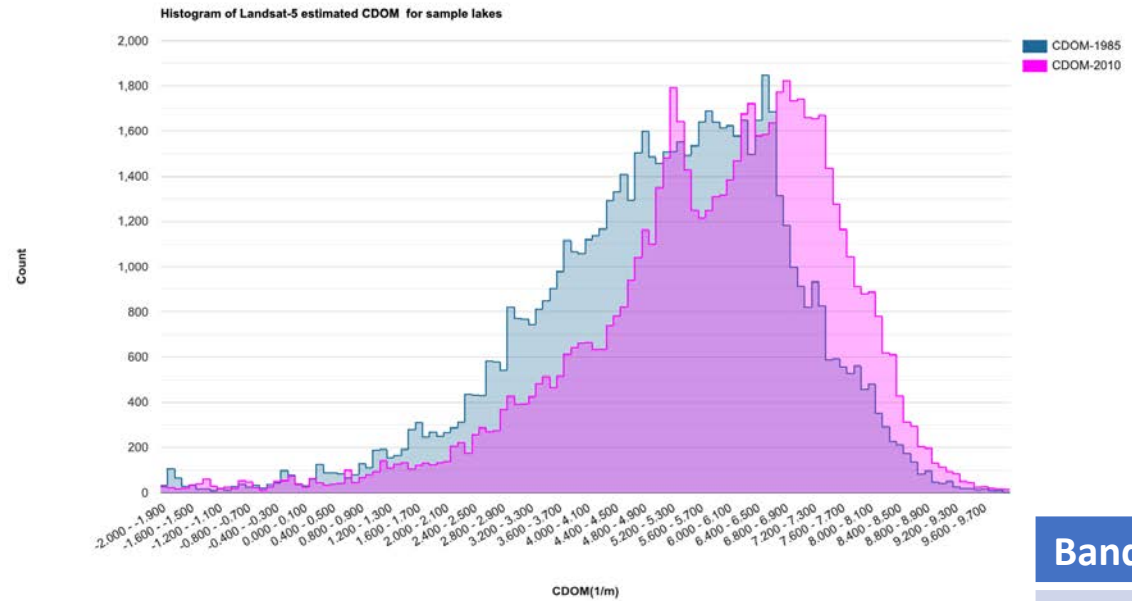
Landsat 7- CDOM difference
2000-2020

Estimated CDOM distribution for ALTM lakes from Landsat 5

Slope of trend for estimated CDOM



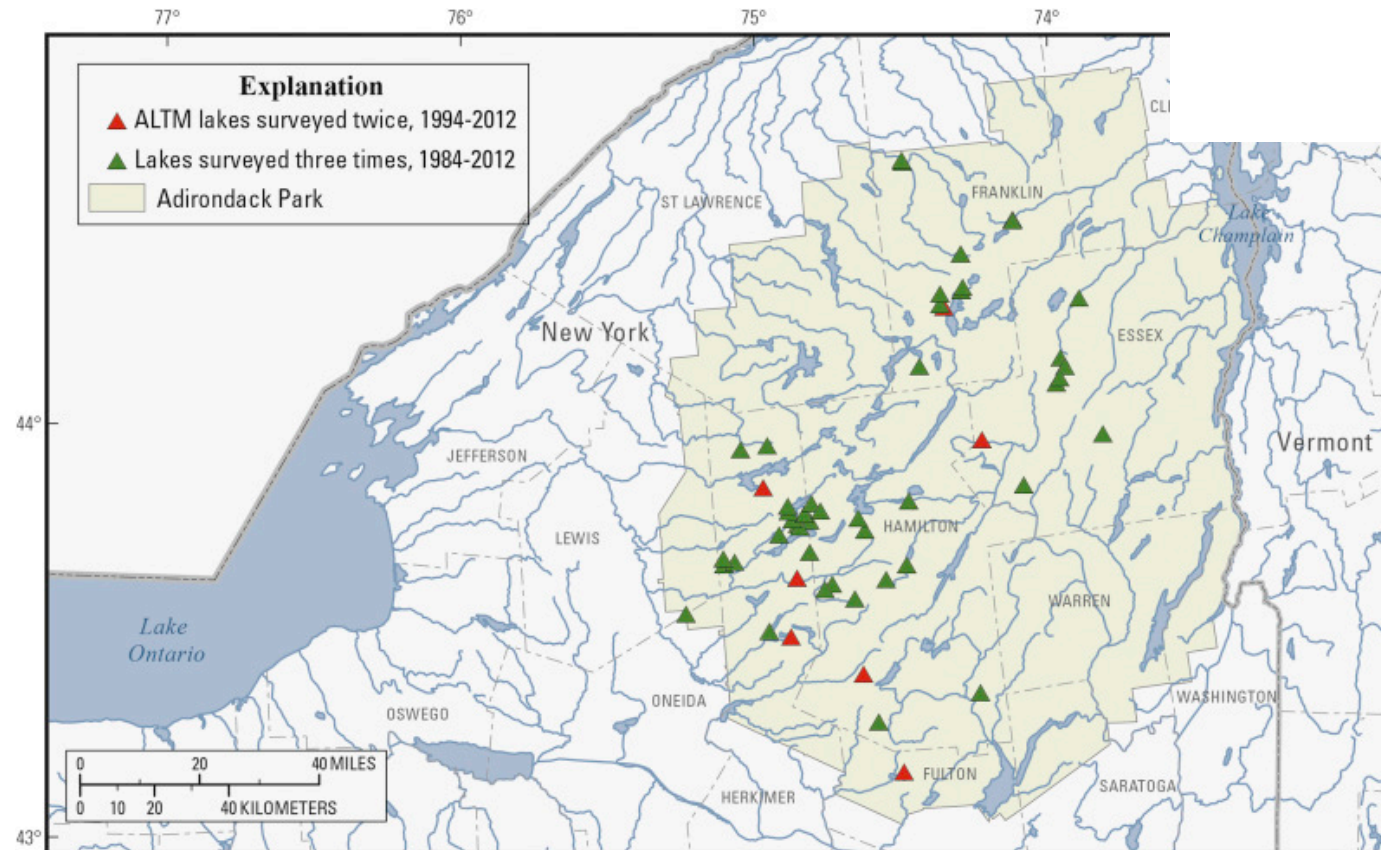
Olamenson et al, 2016 Equation for Landsat 7 is applied on L5
 $CDOM = 20.3 - 10 \cdot (b2/b3) - 2.4 \cdot (b3/b4)$



Band	Color
B1	Blue
B2	Green
B3	Red
B4	NIR

In-Situ data

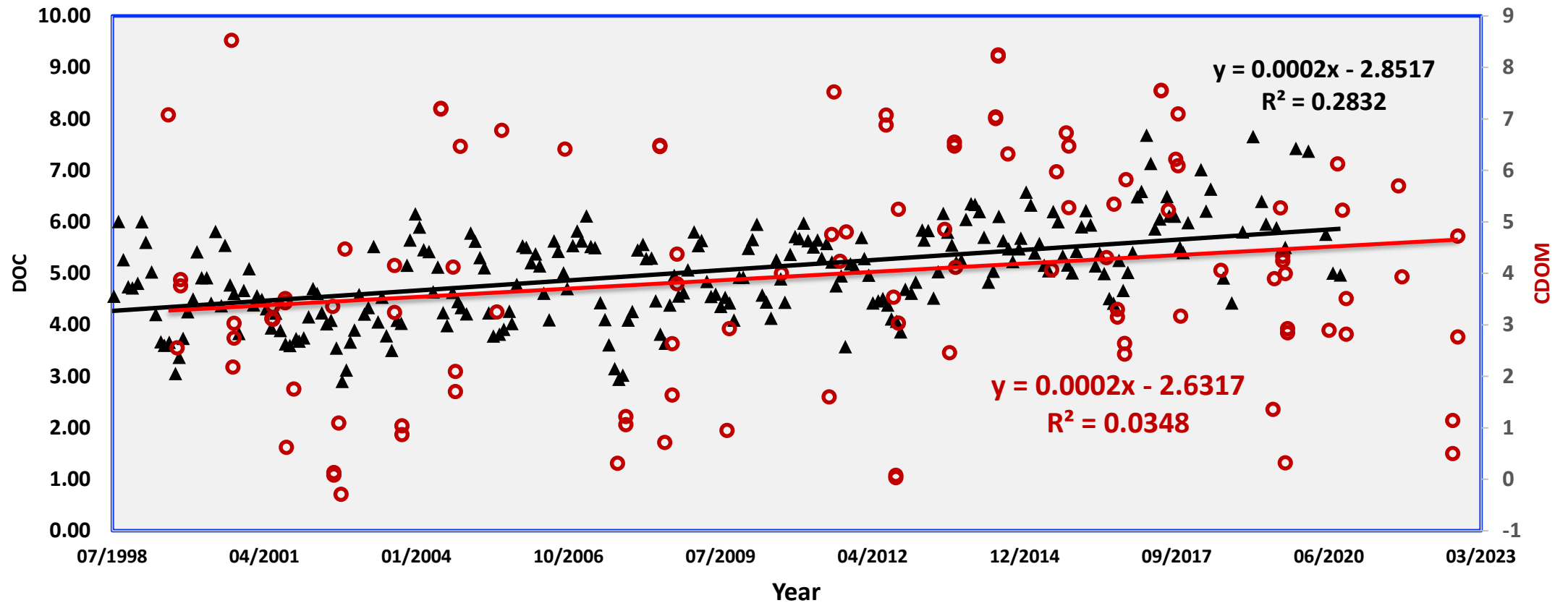
- ALTM
- USGS
- EPA
-



Base from *The National Map*, Universal Transverse Mercator projection, zone 18, WGS84, 1:1,000,000

Trend Analysis

ALTM measured DOC & Landsat-7 estimated CDOM trends over Big Moose Lake



Online Workshops/ Sources

- Fundamentals of Remote Sensing

Register here:

<https://register.gotowebinar.com/register/5234086994456486488>

- Create account on Google Earth Engine
- Watch useful youtube tutorials : Water Quality Monitoring using Remote sensing in Google Earth Engine.

<https://www.youtube.com/live/DLxHS9BgadE?feature=share>

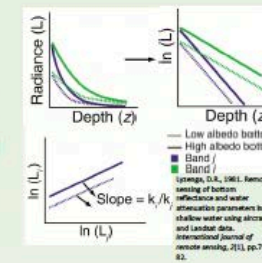
This Video shows some common algorithms used in water quality monitoring.

A UAV based assessment of the distribution of submerged aquatic vegetation in the Upper Hudson River, NY

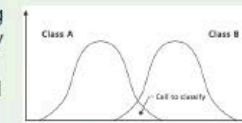


UAV took off and landed on Pontoon Boat and light attenuation values were collected using digital light meter (2nd year) and Secchi Disc

For every CU, illuminance was measured at water surface and at one meter depth. Lux units are converted to Irradiance (W/m²) to calculate attenuation index.



Maximum likelihood method has a strong premise of normality of the distribution of radiance levels for all spectral bands of datasets used to train the classification.

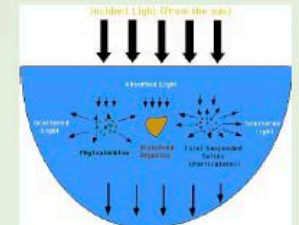


$$\kappa \equiv \frac{p_o - p_e}{1 - p_e} = 1 - \frac{1 - p_o}{1 - p_e}$$

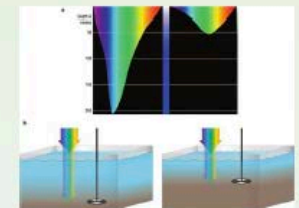
where p_o is the relative observed agreement among raters, and p_e is the hypothetical probability of chance agreement

$$\kappa = \frac{2 \times (TP \times TN - FN \times FP)}{(TP + FP) \times (FP + TN) + (TP + FN) \times (FN + TN)}$$

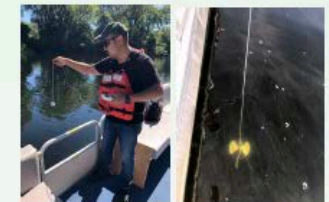
where TP are the true positives, FP are the false positives, TN are the true negatives, and FN are the false negatives



Costeira-Silva, A.J., Lopes-Calcas, A.A., Tejo-Silva, F.C. and Cardine-Betrans, S., 2012. Satellite remote sensing of coral reef habitats mapping in shallow waters at banco chinchorro reefs, Malika: a classification approach. Remote Sensing—Applications, Eschlerer, S., Ed., inTech: Rijak, Croatia, pp.333-354.



Mascarenhas, V. and Kock, T., 2016. Marine optics and ocean color remote sensing. In: OCEANIC 8—Oceans Across Boundaries: Learning from each other: Proceedings of the 2017 conference for YOUNG MARINE RESEARCHERS in Kiel, Germany (pp. 40-54). Springer International Publishing.



Department of Environmental Conservation

